

Binary Solvent-assisted Graphene Synthesis by Direct Exfoliation of Graphite Powder and its Cytotoxicity on SiHa Cell Line

Prabhat Kumar, Purnima Jain, Anjana Sarkar*

Department of Chemistry, Netaji Subhas University of Technology, New Delhi, INDIA.

ABSTRACT

A cost-effective mass production of pristine graphene nanosheet is still an important challenge to harness its maximum potential in medical sciences. Here, we have used a binary solvent mixture of low dielectric constant (1,2,4- trichlorobenzene, $\epsilon = 2.24$ and benzylamine, $\epsilon = 4.6$) to produce a high quantity (0.6 mg/ml) of graphene under ultrasonication without compromising its quality. Obtained sample were characterized through XRD, UV-Vis, Raman, FT-IR, TEM-SAED, and cytopotency was evaluated on SiHa cell line. $I_G/I_{2D} < 1.0$ (~ 0.39) was achieved on more than $250 \mu\text{m}^2$ area, indicating the uniformity and obtained I_D/I_G ratio was 1.21. No toxicity was found in the case of 24 hr on the SiHa cell line. EC_{50} computation was $84.90 \mu\text{g}/\text{ml}$ for 48 hr and $62.03 \mu\text{g}/\text{ml}$ for 72 hr. Exfoliated graphene remained stable in binary solvent even after 1 year. The proposed experiment and obtained data can be powerful tools to explore the synergic effect of binary solvent exfoliation in combination to establish graphene as a biomaterial for neuronal network, tissue engineering, drug delivery, and regenerative medicines, to name a few.

Keywords: Graphene, Nanosheet, Cytotoxicity, SiHa Cell line, Biomaterial.

Submission Date: 10-03-2022;

Revision Date: 07-05-2022;

Accepted Date: 05-06-2022.

INTRODUCTION

Graphene, a well-acclaimed sp^2 hybridized 2D nanomaterials have not only opened the promising new interdisciplinary approach to play a fundamental role for forefront development of nanoelectronics,¹ photonics,² solar power³ harvesting, or flexible ultrathin nanodevice⁴ but also showed its applications in biological systems like the neural network in tissue engineering,⁵ drug delivery⁶ or regenerative medicines⁷ etc. Moreover, high electrical conductivity (10^6 siemens/m),⁸ ultra-high theoretical electron mobility ($10^5 \text{ cm}^2/\text{vs}$),⁹ high visible transmittance (98 %),¹⁰ and excellent mechanical properties (about 1100 GPa)¹¹ make it a suitable candidate for a range of utilizations (Figure 1: Scheme 1: Source of inspiration). Nevertheless, its insolubility and re-aggregation properties have led to either reduced graphene oxide¹² or the chemical vapor deposition

method.¹³ The chemical reduction method introduces defects that completely disrupt the electronic properties by changing the band structure which makes graphene unique while chemical vapor deposition requires a high cost of production with limited outstanding results. The original way of making graphene through mechanical exfoliation introduced by Nobel laureate Sir Andre Geim and Novoselov is insufficient to become a commercial production method.¹⁴ Therefore, to produce high-quality flakes with a large surface area is still restricted commercially, resulting in high demand for an alternative approach for synthesis method which could overcome the conventional issues.

Meanwhile, recent studies have revealed that liquid-phase exfoliation (LPE) of 2D materials has shown a promising approach to obtain monolayer/multilayer

DOI: 10.5530/ijper.56.3.122

Correspondence:

¹Prof. Anjana Sarkar

Department of Chemistry,
Netaji Subhas University of
Technology,
New Delhi-110078, INDIA.
E-mail: anjana.sarkar@nsut.
ac.in

²Mr. Prabhat Kumar

¹Department of Chemistry,
Netaji Subhas University of
Technology,
New Delhi-110078, INDIA.

²Advanced instrumentation
research facility, Jawaharlal
Nehru University,
New Delhi- 110067, INDIA.

E-mail: prabhat.yadav.trf18@
nsut.ac.in



www.ijper.org

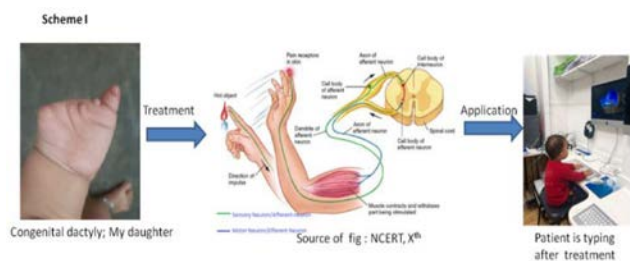


Figure 1: Scheme I. Source of inspiration.

based on dielectric constant and theoretical calculation through first-principle density functional theory (DFT). In this technique, there are three subsequent steps: (1) dispersion of graphite, (2) exfoliation of graphite through ultrasonication, and (3) purification through centrifugation.¹⁵ Physical energy for carrying exfoliation and a solvent as a dispersion medium are pre-requirements in LPE to produce graphene sheets. Cavitation is a process that is employed as physical energy and ultrasonication can be used to generate it,¹⁶ jet cavitation,¹⁷ and high-pressure homogenization¹⁸ can also be used to produce physical energy. Various solvents are used for exfoliation of graphite as well as other 2D nanomaterials like N-methyl pyrrolidone,¹⁹ 1,2-dichlorobenzene,²⁰ benzylamine,²¹ N,N-dimethylformamide,²² dimethylsulfoxide,²³ and γ -butyrolactone, and etc. These solvents attempt were focused on high-quality graphene with significant yield. Nonetheless, literature surveys suggest, yield of graphene in between 0.1-0.3 mg per ml of solvents. However, these findings not only provide an idea about the selection of proper solvent for specific materials but also determines the mechanisms responsible for high yield and defect-free synthesis of graphene. In 2020, Vedanki *et al.* reported a synthesis of pristine graphene by low dielectric constant exfoliating solvent.²⁴ According to this group, chlorobenzene molecule with low dielectric constant refrain from graphene while high dielectric constant propylene carbonate molecule makes a supramolecular bond which leads to produce defects at the edges and basal plane of the nanosheet. Similarly, In 2009, Bourlinos *et al.* outlined several other solvents for exfoliation.²⁵ This group hypothesized that the perfluorinated aromatic molecule works as exfoliating solvent due to π - π interaction across charge transfer because of the presence of electron-withdrawing groups in an aromatic ring. Nevertheless, the quality of graphene is still far behind the theoretical value with a limited commercial approach.

Based on the above hypothesis, this manuscript brings our attempts on further liquid-phase exfoliation

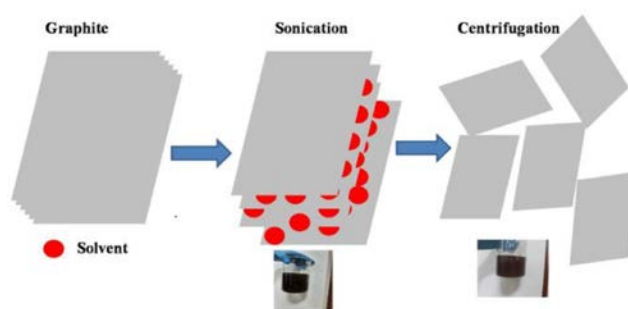


Figure 2: Scheme II. Schematic of exfoliation mechanism.

of graphite powder through binary mixture under ultrasonication. The principal discovery of this work is that an alliance of integrating divergent functional groups having low dielectric constant is more effective in the form of the mixture than a single solvent without adding any surfactant, capping agent or ionic liquid. Few layers graphene dispersed along a high yield of 0.6 mg/ml was synthesized by using the mixture of 1,2,4-trichlorobenzene (dielectric constant, $\epsilon = 2.24$) and benzylamine ($\epsilon = 4.6$) as an exfoliating solvent (Figure 2: Scheme II: Schematic of exfoliation mechanism). The characterization of synthesized graphene samples was performed by XRD, UV-Vis, Raman, FT-IR, and TEM analyses. Additionally, the cytotoxicity of synthesized high-quality graphene samples was illustrated by using the SiHa cell line (human cervical cancer cell line). The experimental results show that binary mixture synthesis of pristine graphene perspective can be a feasible method with a high yield which is one step ahead towards its clinical applications.

MATERIALS AND METHODS

Materials

Graphite powder (purity, 98% C, 50 mesh) was purchased from SRL, Maharashtra, India. 1,2,4-trichlorobenzene and benzylamine were procured from Fisher Scientific, India. 3-(4,5-dimethyl thiazole-2-yl)-2,5-diphenyl tetrazolium bromide (MTT) and Dimethyl sulfoxide, the assay was bought from Sigma Aldrich, USA, and was used as such. Antibodies, trypsin, fetal bovine serum (FBS), and RPMI-1640, the media were procured from GIBCO Island, New York, America. Pure milli-Q water was used as and when required throughout the experiment.

Method of Exfoliation

1.0 g of graphite powder (purity, 98% C, 50 mesh) was put into 100 ml of a binary mixture of 1,2,4-trichlorobenzene and benzylamine in 500 ml of a

flask with continuous stirring for 48 hr. After that, it was sonicated at 400 W, 33 kHz, and 30°C for 2 hr under ultrasonic bath sonicator. After sonication, the dispersion was transferred to falcon tubes and centrifuged for 30 min at 500 rpm. The non-exfoliated portion of graphite was precipitated in the base of falcon tube. The supernatant was decanted carefully and used for further characterizations. A similar method was applied by other scientists.²⁶

Cell culture and MTT assay studies

The cytotoxicity was studied using SiHa cell line (human cervical cancer) procured from the NCCS, DBT, Pune, India. The reduced tetrazolium salt in the MTT assay was examined for cell viability and proliferation with the development of purple color formazan crystals. The cells were preserved in a humidified incubator (37°C, 5% CO₂) and grown with 1 mmol/L sodium pyruvate, 10% (v/v) fetal bovine serum (FBS), and antibiotics (streptomycin 10 µg/mL, penicillin 100 µg/mL) as monolayer in RPMI-1640 medium. In a 96-well plate, SiHa cells (5000 cells/well) were grown and kept for 24 hr. After that, varied concentrations of graphene (12.5 – 100 µg) dissolved in fresh RPMI-1640 media were added to the different grown cells in 96 wells. The formed system was kept for 24 hr, 48 hr, and 72 hr individually. 20 µl of MTT (5 mg/ml) was put in every well before four hours to complete the incubation period. To dissolve the formazan, 200 µl of DMSO was put in to every system after removing the media after completion of the incubation period. The system was again left to grow at room temperature for 10 min. Positive control and blank were used in the experiment.

Characterizations

Synthesized samples were characterized by using X-ray diffraction (XRD), Ultraviolet-visible spectroscopy (UV-Vis), Raman spectroscopy, Fourier transform Infrared rays (FT-IR) spectroscopy, Transmission electron microscopy (TEM), High-resolution transmission electron microscopy (HR-TEM) and selected area electron Diffraction (SAED) pattern. The XRD measurements were performed on graphite powder exfoliated graphene using a PANalytical Xpert Pro system diffractometer (451kV,1401mA) and Cu K α radiation ($\lambda = 1.541781 \text{ \AA}$). The data was obtained in the scattering range of 0°–70° (2 θ) with step size 2° min⁻¹. FT-IR measurement was done On Perkin Elmer of Spectrum two system. UV-Visible absorption spectra were Obtained on UV-2401 PC Shimadzu make through quartz cells of 11cm optical path length. Raman spectrum were recorded from 5501 to 3500 cm⁻¹ using Raman spectrometer (WiTec

α -300 R, Germany) with an SSD laser excitation source (532 nm) at 5 mW applied voltage and 50x magnification objectives. The morphology of the GO and rGO sample was characterized through a transmission electron microscope (TEM JEOL-2100F). The sample was dispersed in water (1 mg/ml) through ultrasonication for 5 min and drop cast on a 200 mesh carbon-coated TEM grid. Ultrasonication was done at 400 W power and 33kHz frequency at room temperature of JAISBO make. Cytotoxicity of exfoliated graphene was evaluated on SiHa cell line (human cervical cancer) using Bio-Rad microplate reader at 595 nm spectral wavelength.

RESULTS AND DISCUSSION

X-Ray Diffraction Analysis

Crystallinity, composition, and interlayer distance (d-spacing) of synthesized nanomaterials were determined by the analysis of obtained XRD pattern. Figure 3, shows the diffraction patterns of graphite and graphene. The well-defined peak (002) of graphite powder was obtained at $2\theta \sim 26.71^\circ$ (JCPDS Card No.-01-075-1621), and the interlayer distance (d-spacing) $\sim 3.33 \text{ \AA}$ was calculated through Bragg's equation, $n\lambda = 2d\sin\theta$. For as-prepared graphene, no peak was observed which is an indication of complete exfoliation of graphite lattice with the successful intercalation of binary mixture between graphite layers. While when the zoomed view of a graph is plotted (inset, Figure 3), we can see the reflection of a very small signature peak at the same point where the graphite peak was present, results in the complete exfoliation of graphite layers.²⁷ Thus, we can achieve crystalline graphene formation after exfoliation. XRD pattern of blank sample holder was performed to confirm the XRD pattern of exfoliated graphene signature peak.

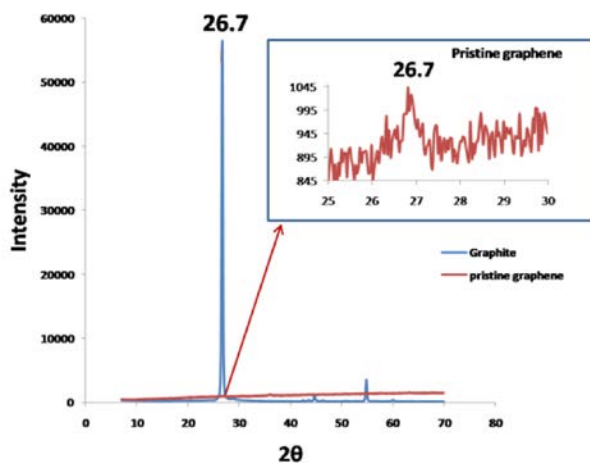


Figure 3: XRD pattern of pure graphite powder and exfoliated graphene.

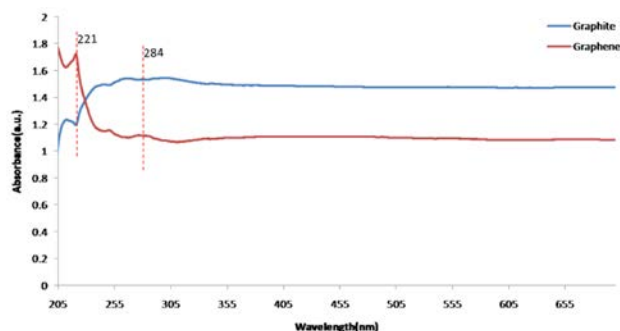


Figure 4: UV – Vis absorption spectra of pure graphite powder and exfoliated graphene.

UV-Vis Measurements

UV-Vis spectra of graphite and graphene are present in Figure 4. The maximum absorption peak for graphene is at 221 nm which correlates the aromatic C-C bonds with $\pi - \pi^*$ transitions. A small hump at 284 nm suggests there is a redshift which can be attributed to the sp^2 hybridized carbon network.²⁸ Absorption is higher in graphite than in graphene is because of the presence of more layered structure.

Raman Measurement

Raman spectroscopy is a non-invasive technique substantially used to investigate the defects, disorders, and number of layers in graphene and its derivatives.²⁹ The positions of Raman peaks, shape, and intensity ratios provide categorical statistics about the number of layers and defects (edges, vacancies, ripples, etc.) present in the graphene lattice. Raman spectra of graphite powder and graphene obtained in the wave number range 1000 cm^{-1} - 3000 cm^{-1} at room temperature are shown in Figure 5. The D-band $\sim 1345\text{ cm}^{-1}$ and the G-band $\sim 1575\text{ cm}^{-1}$ are observed. The G-band originates due to (i) the sp^2 hybridized C=C bond stretching, and (ii) the Brillouin zone occupied by the first-order induced scattering from the doubly generated E_{2g} phonon.³⁰ Therefore, G-band carries detailed information about the sp^2 hybridized carbon network. In contrast, the origin of the D-band is related to the breathing mode of the aromatic rings which is due to excitation of charge carrier and its inelastic scattering by a phonon, second elastic scattering by defects due to oxygen-based functional groups in the carbon basal plane which results in recombination.³¹ D-band, therefore, measures the degree of defects. The presence of a 2D band centered around $2700 - 2900\text{ cm}^{-1}$ is an overtone of the D band and also due to the double resonance transitions. Sharp and single Lorentzian peak can be fitted easily in 2D-band for the monolayer graphene.

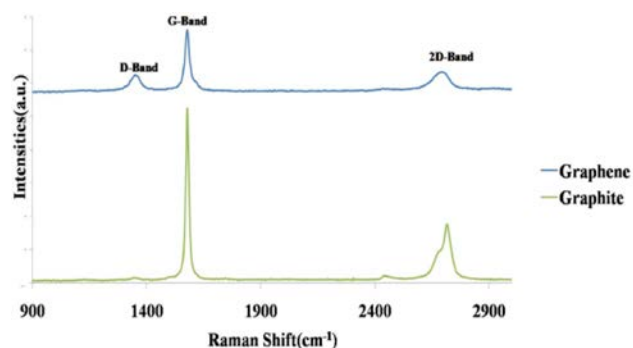


Figure 5: Raman band of pure graphite powder and exfoliated graphene.

The intensity ratio between G-band and 2D band (I_G/I_{2D}), and between D-band and G-band (I_D/I_G) have been measured using confocal Raman imaging. $I_G/I_{2D} < 1.0$ (~ 0.39) was obtained with more than $250\text{ }\mu\text{m}^2$ area of monolayer graphene exfoliated in a binary mixture solvent, suggesting uniformity in the graphene layer. I_D/I_G ratio was found to be 1.21, which suggests some defects incorporated due to exfoliation.³²

FT-IR measurements

FT-IR spectroscopy is like a Raman spectroscopy in which similar kind of vibrational modes, which are present in covalently bonded functional groups of chemical species are sensitive in response to the instrument.³³ Shifts in Raman peaks are whether due to covalent bonding or supra-molecular bonding can be probed through detailed analysis of the FT-IR spectrum of graphene. Ideally, there should not be any significant peak for graphene structure in between $4000 - 400\text{ cm}^{-1}$ with near to 100% transmittance.³⁴ Such a highest transmittance is due to absence of active IR vibrational modes as well as one atom thick and monolayer graphene contains similar atoms. The transmission spectrum of graphene exhibits gentle slope after 3600 cm^{-1} and a steep slope below 2000 cm^{-1} as can be seen in Figure 6. The appearance of such features is because of the effect of intraband shift of free carriers which increases as Fermi energy go away from the Dirac point. Similarly, with the expansion of the graphene layers, Fermi energy shifts towards blue wavelength as Fermi energy is directly related to the number of layers.³⁵ In our case, highest transmittance observed was 90% probably (due to atmospheric effect in exfoliation led to strain development) and decreases as the number of layers increases. Any significant peak suitable to any functional group was absent, but weak bands appeared, which may be due to atmospheric oxidation of thin

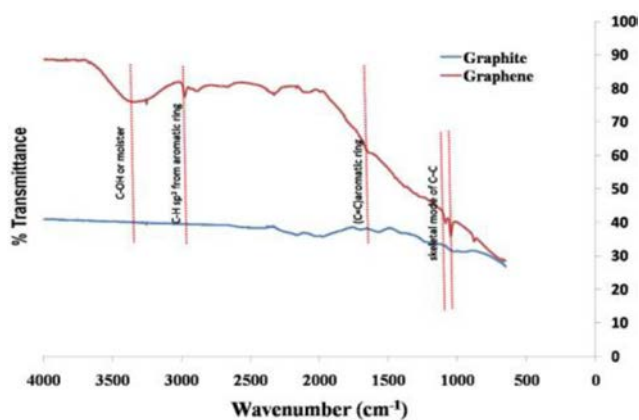


Figure 6: FT - IR spectra of pure graphite powder and exfoliated graphene.

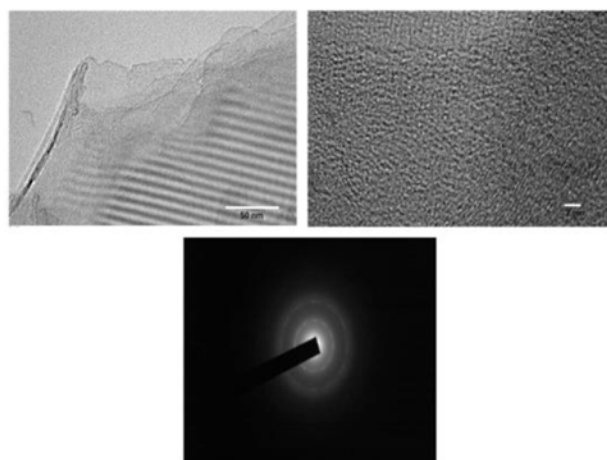


Figure 7: TEM, HR-TEM image and SAED Pattern of exfoliated graphene.

Wavenumber [cm ⁻¹]	Peak allocation	Feature vibration mode for
4000–400	–	no peak for graphene structure
3450–3350	ν (O–H)	–OH from C–OH group or water molecule
3100–3000	ν (=C–H)	–CH from aromatic ring
1680–1630	ν (C=C)	sp ² carbon, aromatic ring
1065	ν (C–C)	skeletal mode of carbon bond

layer graphene and peaks related to aromatic ring and carbon skeletal in the nanosheet (Table 1).

TEM Observation of Obtained few-layer Graphene

HR-TEM image and selected area electron diffraction (SAED) pattern were used to analyze the morphology and crystallinity of the exfoliated graphene as shown in Figure 7. The TEM results of samples project the sheet-like structure having few layers (up to 4 layers). It is worth mentioning here that by increasing the sonication time and optimizing rpm of ultracentrifugation, present Bernal stacked multilayers could be further exfoliated and more monolayer graphene could be obtained.³⁶ Nevertheless, nanosheets are approximately 10 μm in length which is per making better electrical conduction coupled with electrically active nanomaterials. The inset of corresponding TEM images shows the SAED pattern, as can be seen in Figure 5. In the case of the SAED pattern, it is inferred that crystalline regions are present.

Cytopotency

The cell viability, % was calculated using the following formula:

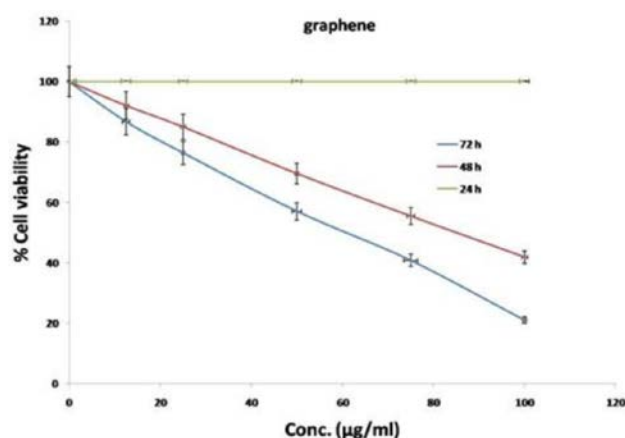


Figure 8: % Viability of SiHa cells treated with different concentration of exfoliated graphene at 24 hr, 48 hr and 72 hr.

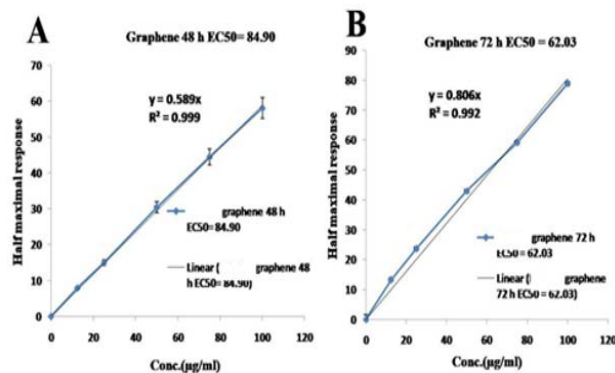


Figure 9: EC₅₀ value of exfoliated graphene at (A) 48 h and (B) 72 h.

$$\% \text{ viability} = \frac{(\text{Mean Optical Density of treated cells})}{(\text{Mean Optical Density of untreated cells, control})} \times 100$$

In Figure 8, the study of cell viability is performed in the range of 0 – 100 μg/ml and EC₅₀ value was

calculated. It was observed that the cell growth inhibition concentration of graphene remained ineffective for 24 hr, while in the case of 48 hr and 72 hr, it showed significant cell growth inhibition concentration. EC_{50} computation was 84.90 $\mu\text{g}/\text{ml}$ for 48 hr and 62.03 $\mu\text{g}/\text{ml}$ for 72 hr (Figure 9). Our demonstrations are in accordance with the previous studies illustrating the cytotoxicity effect of graphene of different compositions.³⁷

CONCLUSION

In summary, solvent exfoliation of graphite to harness graphene monolayers or few layers is a simple without adding any other surfactant/stabilizing/capping/oxidizing agent. A systematic binary solvent (with low dielectric constant, ϵ) exfoliation method under ultrasonication was performed for synthesis. The results revealed important findings concerning the composition, the morphology of 2D nanosheets, and cytotoxicity. XRD pattern showed that graphene was synthesized successfully through exfoliation of graphite powder which could be well correlated with obtained Raman band, TEM images and SAED pattern. Dispersed graphene exhibits stability for up to 1 year. MTT assay studies against the SiHa cell line confirmed the effective concentration of toxicity level and could be further optimized and safely be used in *in vivo* biological activity. Calculated EC_{50} value was 84.90 $\mu\text{g}/\text{ml}$ for 48 hr and 62.03 $\mu\text{g}/\text{ml}$ for 72 hr. The combined results reflected that graphene nanosheets can be optimized as *in-situ* biomaterials applications like tissue engineering, regenerative medicines, targeted drug delivery, etc. Further, the studies related to electrical properties and the *in vivo* of these materials are going on and will be published next.

ACKNOWLEDGEMENT

Financial support for this work was by the Department of Chemistry, Netaji Subhas University of Technology, New Delhi. Prof. Jaydeep Bhattacharya, School of Biotechnology, Jawaharlal Nehru University is highly thankful for various discussions regarding the results part.

CONFLICT OF INTEREST

The authors declare that there is no conflict of interest.

ABBREVIATIONS

XRD: X-Ray diffraction; **UV-Vis:** Ultraviolet-Visible; **FT-IR:** Fourier Transform Infrared spectroscopy;

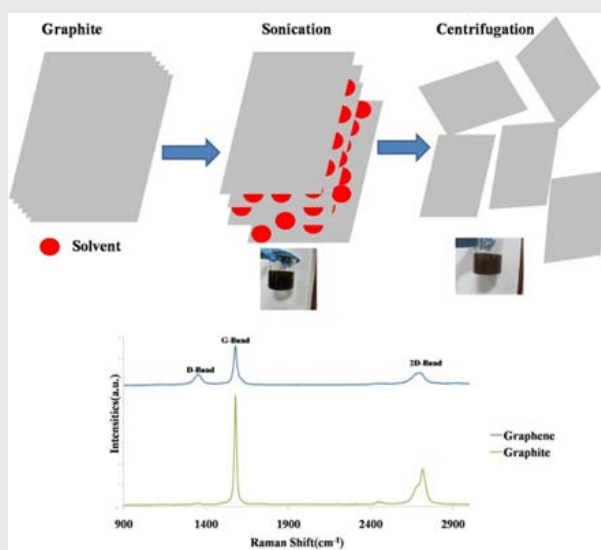
TEM: Transmission electron microscope; **SAED:** Selected area electron diffraction pattern; EC_{50} : half maximal effective concentration; I_G/I_{2D} : Intensity ratio of G-band and 2D band; I_D/I_G : Intensity ratio of G-band and D band; **LPE:** liquid-phase exfoliation; **DFT:** Density functional theory; **MTT:** 3-(4,5-Dimethylthiazol-2-yl)-2,5-Diphenyltetrazolium Bromide; **FBS:** Fetal bovine serum; **RPMI:** Roswell Park Memorial Institute Medium; **NCCS:** National Centre for Cell Science; **DBT:** Department of biotechnology; **DMSO:** Dimethylsulfoxide; **JCPDS:** Joint Committee on Powder Diffraction Standards; **SiHa:** Human cervical cancer cell line.

REFERENCES

1. Radsar T, Khalesi H, Ghods V. Graphene properties and applications in nanoelectronic. *Opt Quant Electron*. 2021 Apr;53(4):1-38. doi: 10.1007/s11082-021-02839-6.
2. Bonaccorso F, Sun Z, Hasan T, Ferrari AC. Graphene photonics and optoelectronics. *Nat Photonics*. 2010 Sep;4(9):611-22. doi: 10.1038/nphoton.2010.186.
3. Iqbal MZ, Rehman AU. Recent progress in graphene incorporated solar cell devices. *Sol Energy*. 2018 Jul 15;169:634-47. doi: 10.1016/j.solener.2018.04.041.
4. Liu Z, Zhao Z, Zeng X, Fu X, Hu Y. Ultrathin, flexible and transparent graphene-based triboelectric nanogenerators for attachable curvature monitoring. *J Phys D: Appl Phys*. 2019 Jun 4;52(31):314002. doi: 10.1088/1361-6463/ab1faa.
5. Baklaushev VP, Bogush VG, Kalsin VA, Sovetnikov NN, Samoilova EM, Revkova VA *et al*. Tissue engineered neural constructs composed of neural precursor cells, recombinant spidroin and PRP for neural tissue regeneration. *Sci Rep*. 2019 Feb 28;9(1):3161. doi: 10.1038/s41598-019-39341-9, PMID 30816182.
6. Sood D, Chwalek K, Stuntz E, Pouli D, Du C, Tang-Schomer M *et al*. Fetal brain extracellular matrix boosts neuronal network formation in 3D bioengineered model of cortical brain tissue. *ACS Biomater Sci Eng*. 2016 Jan 11;2(1):131-40. doi: 10.1021/acsbomaterials.5b00446, PMID 29034320.
7. Kumar S, Chatterjee K. Comprehensive review on the use of graphene-based substrates for regenerative medicine and biomedical devices. *ACS Appl Mater Interfaces*. 2016 Oct 12;8(40):26431-57. doi: 10.1021/acsami.6b09801, PMID 27662057.
8. Kim KS, Zhao Y, Jang H, Lee SY, Kim JM, Kim KS *et al*. Large-scale pattern growth of graphene films for stretchable transparent electrodes. *Nature*. 2009 Feb;457(7230):706-10. doi: 10.1038/nature07719, PMID 19145232.
9. Bolotin KI, Sikes KJ, Jiang Z, Klima M, Fudenberg G, Hone J *et al*. Ultrahigh electron mobility in suspended graphene. *Solid State Commun*. 2008 Jun 1;146(9-10):351-5. doi: 10.1016/j.ssc.2008.02.024.
10. Yadav P, Srivastava PK, Ray N, Ghosh S. Robustness of the universal optical transmittance in monolayer and multilayer graphene flakes under Coulomb interactions. *Phys Rev B*. 2016 Sep 22;94(12):121406. doi: 10.1103/PhysRevB.94.121406.
11. Ovid'Ko IA. Mechanical properties of graphene. *Rev Adv Mater Sci*. 2013 Oct 1;34(1):1.
12. Gómez-Navarro C, Weitz RT, Bittner AM, Scolari M, Mews A, Burghard M *et al*. Electronic transport properties of individual chemically reduced graphene oxide sheets. *Nano Lett*. 2007 Nov 14;7(11):3499-503. doi: 10.1021/nl072090c, PMID 17944526.
13. Zhang YI, Zhang L, Zhou C. Review of chemical vapor deposition of graphene and related applications. *Acc Chem Res*. 2013 Oct 15;46(10):2329-39. doi: 10.1021/ar300203n, PMID 23480816.

14. Novoselov KS, Geim AK, Morozov SV, Jiang D, Katsnelson MI, Grigorieva IV *et al.* Two-dimensional gas of massless Dirac fermions in graphene. *Nature*. 2005 Nov;438(7065):197-200. doi: 10.1038/nature04233, PMID 16281030.
15. Lin PC, Wu JY, Liu WR. Green and facile synthesis of few-layer graphene via liquid exfoliation process for lithium-ion batteries. *Sci Rep*. 2018 Jun 27;8(1):9766. doi: 10.1038/s41598-018-27922-z, PMID 29950565.
16. Lotya M, King PJ, Khan U, De S, Coleman JN. High-concentration, surfactant-stabilized graphene dispersions. *ACS Nano*. 2010 Jun 22;4(6):3155-62. doi: 10.1021/nn1005304, PMID 20455583.
17. Shen Z, Li J, Yi M, Zhang X, Ma S. Preparation of graphene by jet cavitation. *Nanotechnology*. 2011 Aug 16;22(36):365306. doi: 10.1088/0957-4484/22/36/365306, PMID 21844642.
18. Nacken TJ, Damm C, Walter J, Ruger A, Peukert W. Delamination of graphite in a high pressure homogenizer. *RSC Adv*. 2015;5(71):57328-38. doi: 10.1039/C5RA08643D.
19. Hasan T, Scardaci V, Tan P, Rozhin AG, Milne WI, Ferrari AC. Stabilization and "debundling" of single-wall carbon nanotube dispersions in N-methyl-2-pyrrolidone (NMP) by polyvinylpyrrolidone (PVP). *J Phys Chem C*. 2007 Aug 30;111(34):12594-602. doi: 10.1021/jp0723012.
20. Hamilton CE, Lomeda JR, Sun Z, Tour JM, Barron AR. High-yield organic dispersions of unfunctionalized graphene. *Nano Lett*. 2009 Oct 14;9(10):3460-2. doi: 10.1021/nl9016623, PMID 19645460.
21. Cai M, Thorpe D, Adamson DH, Schniepp HC. Methods of graphite exfoliation. *J Mater Chem*. 2012;22(48):24992-5002. doi: 10.1039/C2JM34517J.
22. Blake P, Brimicombe PD, Nair RR, Booth TJ, Jiang D, Schedin F *et al.* Graphene-based liquid crystal device. *Nano Lett*. 2008 Jun 11;8(6):1704-8. doi: 10.1021/nl080649i, PMID 18444691.
23. Du W, Lu J, Sun P, Zhu Y, Jiang X. Organic salt-assisted liquid-phase exfoliation of graphite to produce high-quality graphene. *Chem Phys Lett*. 2013 May 1;568-569:198-201. doi: 10.1016/j.cplett.2013.03.060.
24. Vedanki DC, KumarSrivastava P, Yadav P, Ghosh S. Defect free monolayer and bilayer graphene exfoliated by solvent with low dielectric constant. *AIP Conf Proc*. 2020 Nov 5 (Vol. 2265, No. 1, p. 030713). doi: 10.1063/5.0017671.
25. Bourlinos AB, Georgakilas V, Zboril R, Steriotis TA, Stubos AK. Liquid-phase exfoliation of graphite towards solubilized graphenes *Small*. 2009 Aug 17;5(16):1841-5. doi: 10.1002/sml.200900242, PMID 19408256.
26. Halim U, Zheng CR, Chen Y, Lin Z, Jiang S, Cheng R *et al.* A rational design of cosolvent exfoliation of layered materials by directly probing liquid–solid interaction. *Nat Commun*. 2013 Jul 30;4(1):2213. doi: 10.1038/ncomms3213, PMID 23896793.
27. Lin Y, Jin J, Kusmartsevab O, Song M. Preparation of pristine graphene sheets and large-area/ultrathin graphene films for high conducting and transparent applications. *J Phys Chem C*. 2013 Aug 22;117(33):17237-44. doi: 10.1021/jp403903k.
28. Kartick B, Srivastava SK, Srivastava I. Green synthesis of graphene. *J Nanosci Nanotechnol*. 2013 Jun 1;13(6):4320-4. doi: 10.1166/jnn.2013.7461, PMID 23862494.
29. Ferrari AC. Raman spectroscopy of graphene and graphite: disorder, electron–phonon coupling, doping and nonadiabatic effects. *Solid State Commun*. 2007 Jul 1;143(1-2):47-57. doi: 10.1016/j.ssc.2007.03.052.
30. Ferrari AC, Meyer JC, Scardaci V, Casiraghi C, Lazzeri M, Mauri F *et al.* Raman spectrum of graphene and graphene layers. *Phys Rev Lett*. 2006 Oct 30;97(18):187401. doi: 10.1103/PhysRevLett.97.187401, PMID 17155573.
31. Srivastava PK, Yadav P, Ghosh S. Non-oxidative, controlled exfoliation of graphite in aqueous medium. *Nanoscale*. 2016;8(34):15702-11. doi: 10.1039/C6NR04244A, PMID 27523721.
32. Kastner J, Pichler T, Kuzmany H, Curran S, Blau W, Weldon DN *et al.* Resonance Raman and infrared spectroscopy of carbon nanotubes. *Chem Phys Lett*. 1994 Apr 15;221(1-2):53-8. doi: 10.1016/0009-2614(94)87015-2.
33. Hu H, Liao B, Guo X, Hu D, Qiao X, Liu N *et al.* Large-scale suspended graphene used as a transparent substrate for infrared spectroscopy. *Small*. 2017 Jul;13(25):1603812. doi: 10.1002/sml.201603812, PMID 28508534.
34. Rodrigo D, Tittl A, Limaj O, Abajo FJG, Pruneri V, Altug H. Double-layer graphene for enhanced tunable infrared plasmonics. *Light Sci Appl*. 2017 Jun;6(6):e16277-. doi: 10.1038/lsa.2016.277, PMID 30167262.
35. Srivastava PK, Yadav P, Ghosh S. Dielectric environment as a factor to enhance the production yield of solvent exfoliated graphene. *RSC Adv*. 2015;5(79):64395-403. doi: 10.1039/C5RA12464F.
36. Yadav P, Srivastava PK, Ghosh S. Dielectric screening of excitons in monolayer graphene. *Nanoscale*. 2015;7(43):18015-9. doi: 10.1039/C5NR04800A, PMID 26469682.
37. Lasocka I, Szulc-Dąbrowska L, Skibniewski M, Skibniewska E, Gregorczyk-Zboroch K, Pasternak I *et al.* Cytocompatibility of graphene monolayer and its impact on focal cell adhesion, mitochondrial morphology and activity in BALB/3T3 fibroblasts. *Materials (Basel)*. 2021 Jan;14(3):643. doi: 10.3390/ma14030643, PMID 33573304.

PICTORIAL ABSTRACT



SUMMARY

- A binary solvent was used to successfully exfoliate graphite powder into graphene.
- For monolayer graphene, IG/I2D < 1.0 (~ 0.39) was found on more than 250 μm^2 area of graphene, indicating the uniformity of the graphene layer. ID/IG ratio was found to be 1.21.
- Few layer graphene dispersed with a high concentration of 0.6 mg/ml was prepared by using the mixture of 1,2,4-trichlorobenzene (dielectric constant, $\epsilon = 2.24$) and benzylamine ($\epsilon = 4.6$) as an exfoliating solvent.
- No toxicity was found for exfoliated graphene in the case of 24 h on the SiHa cell line.
- The EC_{50} computation for exfoliated graphene was 84.90 $\mu\text{g}/\text{ml}$ for 48 h and 62.03 $\mu\text{g}/\text{ml}$ for 72 h.
- Exfoliated graphene remained stable in binary solvent even after 1 year.

About Authors

Prabhat Kumar is serving as a teaching cum research fellow (TRF- PhD), in the Department of Chemistry, Netaji Subhas University of Technology, New Delhi, India. His areas of interest are biomaterials, drug discovery and carcinogenesis. He attained M.S. degree in Materials Chemistry from School of Materials Science, Japan Advanced Institute of Science and Technology (JAIST), Ishikawa, Japan and M.Tech. degree in Chemical Synthesis and Process Technologies from Department of Chemistry, University of Delhi, New Delhi, India. He worked as a Research Associate in Jawaharlal Nehru University, New Delhi, India for 6 years in Department of Biotechnology (DBT) project. He is active in research and has more than 15 international and national research publications to his credit. Besides this, he is a reviewer in the journal of Carcinogenesis, Oxford University Press and Indian journal of pharmaceutical education and research, Bangalore, India.

Prof. Purnima Jain is serving as a professor in the Department of Chemistry, Netaji Subhas University of Technology, New Delhi, India. She completed her Master of Science and Master of Technology from department of Chemistry, IIT Delhi, India and Ph.D. from Centre for Polymer Science and Technology IIT Delhi, India. Besides teaching chemistry her general research interests are development and characterization of blends, alloys and nanocomposites of polymers

Prof. Anjana Sarkar is serving as a professor and HoD in the Department of Chemistry, Netaji Subhas University of Technology, New Delhi, India. She completed her Master of Science in Organic Chemistry from department of Chemistry, Calcutta University, West Bengal, India and Ph.D. from Department of Chemistry, University of Delhi, New Delhi, India. Besides teaching her research areas of interest are organic chemistry. She had served as a Principal Investigator of AICTE sponsored R&D Project: Ternary Complexes of Transition Metal Ions with Novel Biomolecular like Kojic Acid & L-Amino acid : Synthesis & Study of Physicochemical Properties and their Bio-efficacy. She has been awarded "Woman of the Year 1998." By The American Biographical Institute, North Carolina. USA.

Cite this article: Kumar P, Jain P, Sarkar A. Binary Solvent-assisted Graphene Synthesis by Direct Exfoliation of Graphite Powder and its Cytotoxicity on SiHa Cell Line. Indian J of Pharmaceutical Education and Research. 2022;56(3):732-9.